JOC Article

Solution-Processable Stiff Dendrimers: Synthesis, Photophysics, Film Morphology, and Electroluminescence

Zujin Zhao,[†] Juo-Hao Li,[‡] Xiaopeng Chen,[†] Xiaoming Wang,[†] Ping Lu,*[,†] and Yang Yang*[,‡]

Department of Chemistry, Zhejiang University, Hangzhou 310027, People's Republic of China, and Department of Materials Science and Engineering, University of California, Los Angeles, California 90095

pinglu@zju.edu.cn; yangy@ucla.edu

Received October 9, 2008

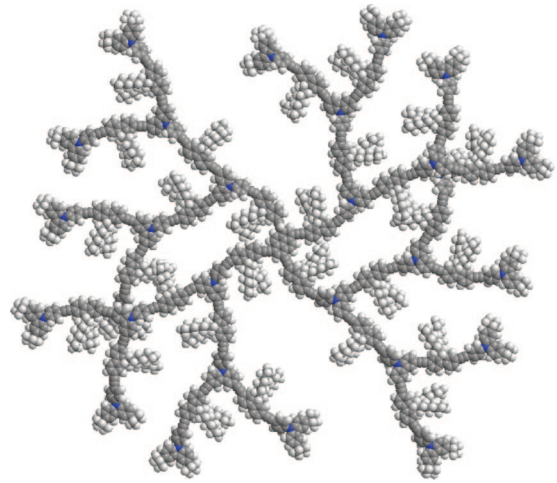

A series of solution-processable conjugated dendrimers (**T1**−**T5**) consisting of a pyrene core, fluorene/carbazole dendrons, and acetylene linkages have been successfully synthesized and fully characterized. The effects of generation on the photoluminescence (PL) and electroluminescence (EL) of dendrimers are investigated. Photon harvest and energy transfer are observed in these dendritic systems. Efficient electroluminescent single layer dendrimer devices are achieved through control of dendrimer generation and optimization of spin-coating speed. A **T3**-based device exhibits yellow EL (CIE: 0.49, 0.50) with a maximum brightness of 5590 cd/m^2 at 16 V, a high current efficiency of 2.67 cd/A at 8.6 V, and a best external quantum efficiency of 0.86%.

1. Introduction

In the field of organic light-emitting diodes (OLEDs), great effort has been made on developing new materials as well as optimizing device architectures to realize full-color, flat-panel displays with improved efficiency and lifetime.[1] Two classes of materials, small molecules and conjugated polymers, have received the most attention in the past two decades. Small organic molecules with well-defined structures and excellent purity are generally processed by thermal evaporation under high vacuum, developed by Tang and VanSlyke,[2] while fluorescent polymers, discovered at Cambridge,[3] may be deposited directly from solution by simple processes such as spin-coating and ink-jet printing.[4] Besides small molecules and polymers, a new class of materials, light-emitting dendrimers, is becoming prominent in OLEDs recently.[5] Dendrimers are hyperbranched macromolecules combining the merits of well-defined structures and superior chemical purity possessed by small molecules and

[†] Zhejiang University.
[‡] University of California.

(1) (a) D'Andrade, B. W.; Forrest, S. R. *Adv. Mater.* **2004**, *16*, 1585. (b) Chen, C.-T. *Chem, Mater.* **2004**, *16*, 4389. (c) Shih, P.-I.; Tseng, Y.-H.; Wu, F.-I.; Dixit, A. K.; Shu, C.-F. *Adv. Funct. Mater.* **2006**, *16*, 1582.

(2) Tang, C. W.; van Slyke, S. A. *Appl. Phys. Lett.* **1987**, *51*, 913.

(3) Burroughes, J. H.; Bradley, D. D. C.; Brown, A. R.; Marks, R. N.; Mackay, K.; Friend, R. H.; Burn, P. L.; Holmes, A. B. *Nature* **1990**, *347*, 539.

(4) (a) Yang, Y.; Chang, S. C.; Bharathan, J.; Liu, J. *J. Mater. Sci.: Mater. Electron.* **2000**, *11*, 89. (b) de Gans, B. J.; Schubert, U. S. *Macromol. Rapid Commun.* **2003**, *24*, 659.

10.1021/jo802237c CCC: $40.75 © 2009 American Chemical Society
Published on Web 11/19/2008

simple solution-processing advantage of polymers.[6] The well-designed and controlled molecular synthesis of dendrimers can offer desired properties, such as formation of high-quality amorphous film by the simple spin-coating method,[7] emission enhancement via energy transfer from peripheries to the emitting core,[8] suppression of aggregates and fluorescence quenching by encapsulating the emitting segment,[9] and tunable charge transport ability through generation control.[10] Moreover, the ability to easily tune the size, topology, molecular weight, and consequently the properties of the dendrimers has led to their widespread use in a variety of applications from material to biology science.[11]

So far, a great many of dendrimers have been synthesized and studied, such as dendrimers with stilbene dendrons,[6,9a,c,d,12] and dendrimers with poly(benzyl ether) dendrons.[5e,f,13] For acetylene-linked dendrimers, Moore[14] reported the first fluorescent dendrimers consisting of a 9,10-(diphenylacetylenyl)anthracene chromophore and triphenylamine-containing dendrons. The performances of LEDs utilizing them as emitting-layers are relatively poor. Later, Jin[15] reported dendrimers with the same core but with 1,3,4-oxadiazole-containing dendrons. However, no significant improvement in the EL efficiency is observed. The poor EL properties of these materials are ascribed to the acetylene linkages, which allow the dendrimers to adopt a more planar structure. The enhancement in planarity will induce stronger intermolecular interactions between chromophores, resulting in nonradiative decay of excitons. Therefore, dendrimers with acetylene linkages are considered as unpromising light-emitting materials[5c] and only a few reports are available in the literature. Nevertheless, in our opinion, although $\pi-\pi$ stacking between aromatic chromophores can result in luminescence quenching accompanied by a red-shift in emission, it can lead to higher charge transport. In this regard, if we can have a good control on the degree of intermolecular interactions to balance the negative and positive factors, the acetylene-linked dendrimers may emit strong EL with high efficiency.

In this paper, we report the synthesis and characterization of a new series of acetylene-linked dendrimers inspired from Moore's models.[16] Polycyclic aromatic pyrene is chosen as a chromophoric core of stiff dendrimers because of its excellent PL efficiency,[17] high carrier mobility, and wide use of its derivatives as active layers in field effect transistors (FETs)[18] and OLEDs.[19] Moreover, it allows researchers to study the generation effect on the aggregation of dendrimers[20] because pyrenes are prone to excimer formation in concentrated solutions and in solid states.[21] On the basis of our previous work,[22] strong blue fluorescent carbazole/fluorene combinations are chosen as dendrons. This is because carbazole possesses good hole transport ability and can be easily modified at its 3-, 6-, and 9-positions.[23] Meantime, efficient energy harvest and transfer are observed in carbazole-based dendrons,[24] and the singlet and triplet energy of carbazole can be transferred to the core, affording a high EL efficiency.[25] Fluorene is a blue chromophore that can also be utilized to construct dendrimers with desired characteristics and usage.[26] Here, the bis(*n*-heptyl)-substituted fluorenes embedded in the dendrons can extend the dendrimer

(5) (a) Howard, W. E. *Sci. Am.* **2004**, *290*, 64. (b) Holder, E.; Langeveld, B. M. W.; Schubert, U. S. *Adv. Mater.* **2005**, *17*, 1109. (c) Burn, P. L.; Lo, S.-C.; Samuel, I. D. W. *Adv. Mater.* **2007**, *19*, 1675. (d) Anthopoulos, T. D.; Frampton, M. J.; Namdas, E. B.; Burn, P. L.; Samuel, I. D. W. *Adv. Mater.* **2004**, *16*, 557. (e) Furuta, P.; Brooks, J.; Thompson, M. E.; Fréchet, J. M. J. *J. Am. Chem. Soc.* **2003**, *125*, 13165. (f) Freeman, A. W.; Koene, S. C.; Malenfant, P. R. L.; Thompson, M. E.; Fréchet, J. M. J. *J. Am. Chem. Soc.* **2000**, *122*, 12385. (g) Kwon, T. W.; Alam, M. M.; Jenekhe, S. A. *Chem, Mater.* **2004**, *16*, 4657. (h) Choi, D. H.; Han, K.; Chang, I.-H.; Zhang, X.-H.; Ahn, K.-H.; Lee, Y. K.; Jang, J. *Synth. Met.* **2007**, *157*, 332. (i) Bolink, H. J.; Barea, E.; Costa, R. D.; Coronado, E.; Sudhakar, S.; Zhen, C.; Sellinger, A. *Org. Electron.* **2008**, *9*, 155.

(6) (a) Lupton, J. M.; Samuel, I. D. W.; Beavington, R.; Burn, P. L.; Bässler, H. *Adv. Mater.* **2001**, *13*, 258. (b) Frampton, M. J.; Beavington, R.; Samuel, I. D. W.; Burn, P. L. *Synth. Met.* **2001**, *121*, 1671. (c) Ma, D.; Hu, Y.; Zhang, Y.; Wang, L.; Jing, X.; Wang, F.; Lupton, J. M.; Samuel, I. D. W.; Lo, S.-C.; Burn, P. L. *Synth. Met.* **2003**, *137*, 1125. (d) Pillow, J. N. G.; Halim, M.; Lupton, J. M.; Burn, P. L.; Samuel, I. D. W. *Macromolecules* **1999**, *32*, 5985.

(7) (a) Lai, W.-Y.; Zhu, R.; Fan, Q.-L.; Hou, L.-T.; Cao, Y.; Huang, W. *Macromolecules* **2006**, *39*, 3707. (b) Sun, Y.; Xiao, K.; Liu, Y.; Wang, J.; Pei, J.; Yu, G.; Zhu, D. *Adv. Funct. Mater.* **2005**, *15*, 818.

(8) (a) Chen, C.-H.; Lin, J. T.; Yeh, M.-C. P. *Org. Lett.* **2006**, *8*, 2233. (b) Goodson, T. *Acc. Chem. Res.* **2005**, *38*, 99. (c) Goodson, T. *Annu. Rev. Phys. Chem.* **2005**, *56*, 581. (d) Kawa, M.; Takahagi, T. *Chem. Mater.* **2004**, *16*, 2282. (e) Zhu, L.; Tong, X.; Li, M.; Wang, E. *J. Phys. Chem. B* **2001**, *105*, 2461. (f) Wang, J.-L.; Yan, J.; Tang, Z.-M.; Xiao, Q.; Ma, Y.; Pei, J. *J. Am. Chem. Soc.* **2008**, *130*, 9952.

(9) (a) Halim, M.; Pillow, J. N. G.; Burn, P. L.; Samuel, I. D. W. *Adv. Mater.* **1999**, *11*, 371. (b) Pålsson, L.-O.; Beavington, R.; Frampton, M. J.; Lupton, J. M.; Magennis, S. W.; Markham, J. P. J.; Pillow, J. N. G.; Burn, P. L.; Samuel, I. D. W. *Macromolecules* **2002**, *35*, 7891. (c) Markham, J. P. J.; Lo, S.-C.; Magennis, S. W.; Burn, P. L.; Samuel, I. D. W. *Appl. Phys. Lett.* **2002**, *80*, 2645. (d) Kwok, C. C.; Wong, M. S. *Macromolecules* **2001**, *34*, 6821.

(10) (a) Burn, P. L.; Halim, M.; Pillow, J. N. G.; Samuel, I. D. W. *SPIE* **1999**, *3797*, 66. (b) Lupton, J. M.; Samuel, I. D. W.; Beavington, R.; Burn, P. L.; Bässler, H. *Adv. Mater.* **2001**, *13*, 258. (c) Lupton, J. M.; Samuel, I. D. W.; Beavington, R.; Frampton, M. J.; Burn, P. L.; Bässler, H. *Phys. Rev. B* **2001**, *63*, 155206.

(11) (a) Newkome, G. R.; Moorefield, C. N.; Vögtle, F. *Dendrimers and Dendrons*, Wiley-VCH: Weinheim, Germany, 2001. (b) Fréchet, J. M. J.; Tomalia, D. A., Eds. *Dendrimers and Other Dendritic Polymers*; Wiley-VCH: Chichester, UK, 2001. (c) Tomalia, D. A.; Fréchet, J. M. J. *Prog. Polym. Sci.* **2005**, *30*, 217. (d) Majoral, J.-P. *New J. Chem.* **2007**, *31*, 1039.

(12) García-Martínez, J. C.; Díez-Barra, E.; Rodríguez-López, J. *Curr. Org. Synth.* **2008**, *5*, 267.

(13) (a) Hecht, S.; Fréchet, J. M. J. *Angew. Chem., Int. Ed.* **2001**, *40*, 74. (b) Freeman, A. W.; Fréchet, J. M. J.; Koene, S. C.; Thompson, M. E. *Polym. Prepr. (Am. Chem. Soc. Div. Polym. Chem.)* **1999**, *40*, 1246. (c) Koene, S. C.; Freeman, A. W.; Killeen, K. A.; Fréchet, J. M. J.; Thompson, M. E. *Polym. Mater. Sci. Eng.* **1999**, *80*, 238.

(14) Wang, P. W.; Liu, Y. J.; Decadoss, C.; Bharathi, P.; Moore, J. S. *Adv. Mater.* **1996**, *8*, 237.

(15) Cha, S. W.; Choi, S.-H.; Kim, K.; Jin, J.-I. *J. Mater. Chem.* **2003**, *13*, 1900.

(16) Devadoss, C.; Bharathi, P.; Moore, J. S. *J. Am. Chem. Soc.* **1996**, *118*, 9635.

(17) Bevilacqua, P. C.; Kierzek, R.; Johnson, K. A.; Turner, D. H. *Science* **1992**, *258*, 1355.

(18) (a) Moggia, F.; Videlot-Ackermann, C.; Ackermann, J.; Raynal, P.; Brisset, H.; Fages, F. *J. Mater. Chem.* **2006**, *16*, 2380. (b) Zhang, H.; Wang, Y.; Shao, K.; Liu, Y.; Chen, S.; Qiu, W.; Sun, X.; Qi, T.; Ma, Y.; Yu, G.; Su, Z.; Zhu, D. *Chem. Commun.* **2006**, 755.

(19) (a) Tao, S.; Peng, Z.; Zhang, X.; Wang, P.; Lee, C.-S.; Lee, S.-T. *Adv. Funct. Mater.* **2005**, *15*, 1716. (b) Tang, C.; Liu, F.; Xia, Y.-J.; Wei, A.; Li, S.-B.; Fan, Q.-L.; Huang, W. *J. Mater. Chem.* **2006**, *16*, 4074. (c) Cirpan, A.; Rathnayake, H. P.; Lahti, P. M.; Karasz, F. E. *J. Mater. Chem.* **2007**, *17*, 3030. (d) Zhao, Z.; Zhang, P.; Wang, F.; Wang, Z.; Lu, P.; Tian, W. *Chem. Phys. Lett.* **2006**, *423*, 293. (e) Zhao, Z.; Li, J.-H.; Lu, P.; Yang, Y. *Adv. Funct. Mater.* **2007**, *17*, 2203. (f) Zhao, Z.; Xu, X.; Jiang, Z.; Lu, P.; Yu, G.; Liu, Y. *J. Org. Chem.* **2007**, *72*, 8345. (g) Hancock, J. M.; Gifford, A. P.; Tonzola, C. J.; Jenekhe, S. A. *J. Phys. Chem. C* **2007**, *111*, 6875.

(20) Bernhardt, S.; Kastler, M.; Enkelmann, V.; Baumgarten, M.; Müllen, K. *Chem. Eur. J.* **2006**, *12*, 6117.

(21) (a) Venkataramana, G.; Sankararaman, S. *Org. Lett.* **2006**, *8*, 2739. (b) Nandy, R.; Subramoni, M.; Varghese, B.; Sankararaman, S. *J. Org. Chem.* **2007**, *72*, 938.

(22) (a) Zhao, Z.; Xu, X.; Chen, X.; Wang, X.; Lu, P.; Yu, G.; Liu, Y. *Tetrahedron* **2008**, *64*, 2658. (b) Zhao, Z.; Li, J.-H.; Chen, X.; Lu, P.; Yang, Y. *Org. Lett.* **2008**, *10*, 3041.

(23) (a) Zhu, Z.; Moore, J. S. *J. Org. Chem.* **2000**, *65*, 116. (b) Zhu, Z.; Moore, J. S. *Macromolecules* **2000**, *33*, 801.

(24) (a) Loiseau, F.; Campagna, S.; Hameurlaine, A.; Dehaen, W. *J. Am. Chem. Soc.* **2005**, *127*, 11352. (b) Wong, K.-T.; Lin, Y.-H.; Wu, H.-H.; Fungo, F. *Org. Lett.* **2007**, *9*, 4531.

(25) (a) Ding, J.; Gao, J.; Cheng, Y.; Xie, Z.; Wang, L.; Ma, D.; Jing, X.; Wang, F. *Adv. Funct. Mater.* **2006**, *16*, 575. (b) Kwon, T.-H.; Kim, M. K.; Kwon, J.; Shin, D.-Y.; Park, S. J.; Lee, C.-L.; Kim, J.-J.; Hong, J.-I. *Chem. Mater.* **2007**, *19*, 3673.

(26) (a) Sun, M.; Li, J.; Li, B.; Fu, Y.; Bo, Z. *Macromolecules* **2005**, *38*, 2651. (b) Wang, S.; Gaylord, B. S.; Bazan, G. C. *Adv. Mater.* **2004**, *16*, 2127. (c) Mongin, O.; Krishna, T. R.; Werts, M. H. V.; Caminade, A.-M.; Majoral, J.-P.; Blanchard-Desce, M. *Chem. Commun.* **2006**, 915.

SCHEME 1[a]

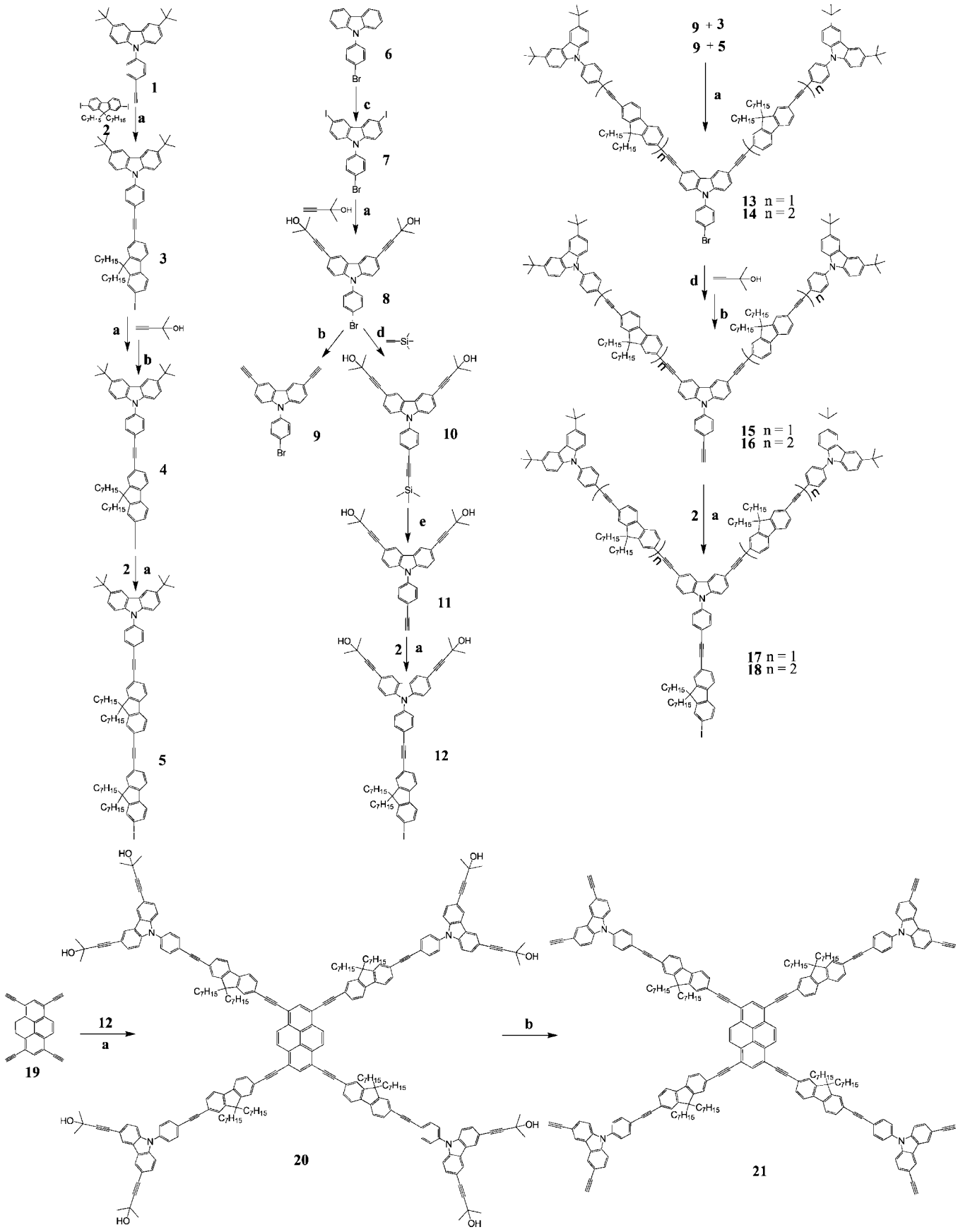

[a] Conditions and reagents: (a) $Pd(PPh_3)_2Cl_2$, PPh_3, CuI, Et_3N, N_2, reflux. (b) KOH, 2-propanol, reflux. (c) KI, KIO_3, acetic acid, 80 °C. (d) $Pd(PPh_3)_4$, PPh_3, CuI, *i*-Pr_2NH, N_2, reflux. (e) *n*-Bu_4NF, THF, rt.

SCHEME 2[a]

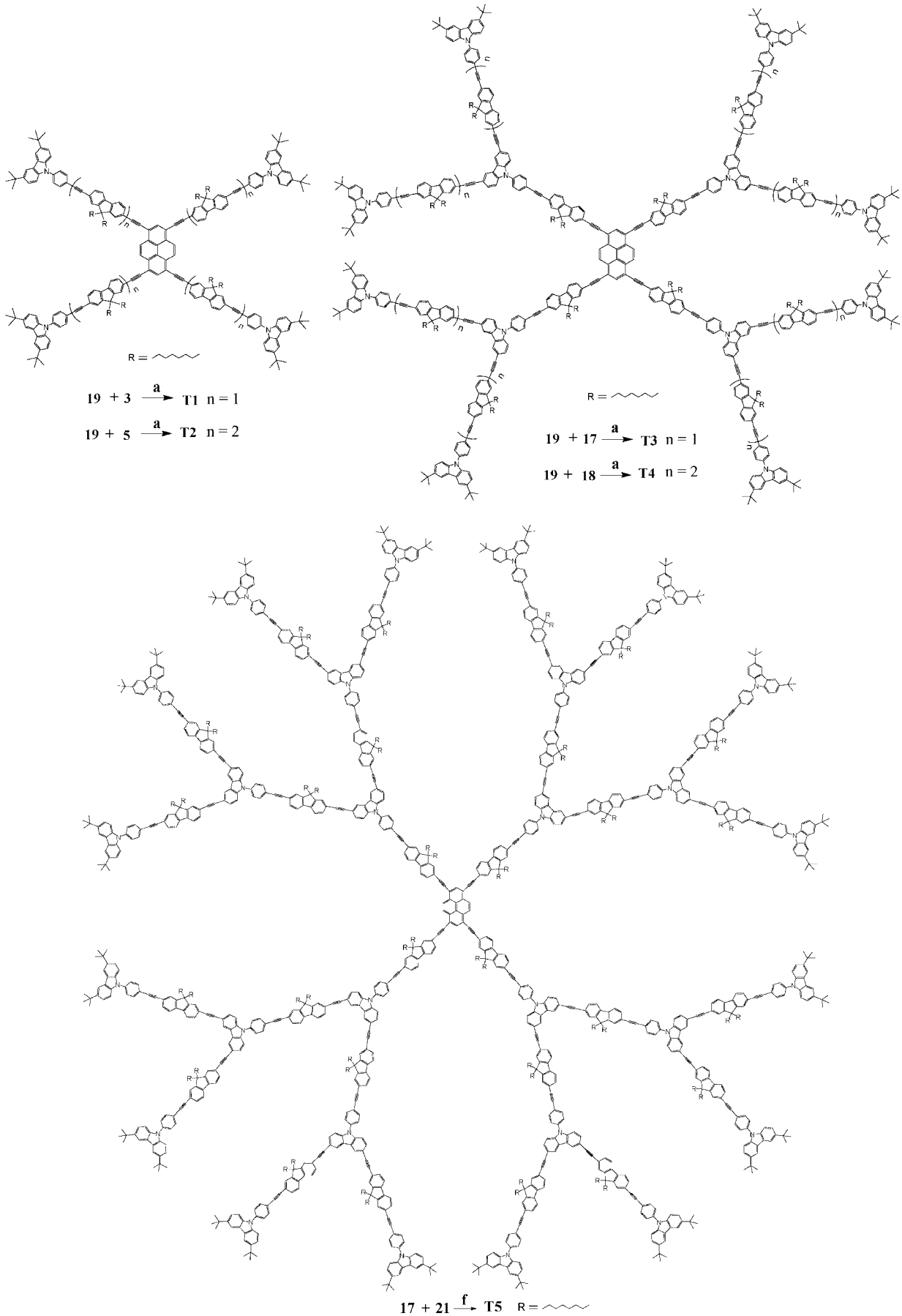

[a] Conditions and reagents: (a) $Pd(PPh_3)_2Cl_2$, PPh_3, CuI, Et_3N, N_2, reflux. (f) $Pd(PPh_3)_4$, PPh_3, CuI, *i*-Pr_2NH/benzene (1/1, v/v), N_2, reflux.

TABLE 1. Optical, Electrochemical, and Thermal Properties of Dendrimers T1−T5

	CH_2Cl_2			film					
	λ_{abs} (nm) ($\varepsilon \times 10^5$)[a]	λ_{em} (nm)	Φ	λ_{abs} (nm)	λ_{em} (nm)	E_g[b] (eV)	E^{ox}_{onset}[c] (V)	HOMO/LUMO (eV)	T_g/T_d (°C)
T1	395 (2.4), 474 (0.9), 501 (1.0)	523 (560)	0.58	397, 478, 506	531, 572	2.35	1.58	−5.98/−3.62	154/436
T2	381 (3.8), 401 (4.0), 476 (0.9), 503 (1.0)	525 (553)	0.65	378, 402, 478, 507	532, 568	2.35	1.52	−5.92/−3.56	128/431
T3	374 (9.1), 390 (9.0), 475 (0.9), 501 (1.0)	523 (559)	0.48	368, 478, 503	558	2.35	1.49	−5.89/−3.53	174/442
T4	383 (14.9), 401 (14.1), 475 (0.9), 501 (1.0)	(414) (440) 523 (560)	0.46	382, 479, 503	562	2.35	1.46	−5.86/−3.51	160/439
T5	376 (20.1), 390 (19.9), 476 (0.9), 501 (1.0)	(405) 522 (558)	0.42	370, 476, 504	530	2.35	1.36	−5.76/−3.41	161/425

[a] Mole absorption coefficient (ε): M^{-1} cm^{-1}, within an error of $\pm 0.1 \times 10^5$ M^{-1} cm^{-1}. [b] Energy band gap determined from UV−vis absorption spectra. [c] E^{ox}_{onset} = onset oxidation potential; potentials vs Ag/AgCl, working electrode Pt, 0.1 M Bu_4NPF_6−CH_2Cl_2, scan rate 100 mV/s.

molecules, and afford a good solubility and better film-forming property. On the basis of the synthesized dendrimers, the effects of generations on the PL and EL of dendrimers are demonstrated. Moreover, the influence of spin-coating speed on the performances of dendrimer LED is investigated.

2. Results and Discussion

2.1. Synthesis. Schemes 1 and 2 illustrate the synthetic routes of intermediates and final dendrimers. A Pd/Cu-catalyzed Sonogashira coupling reaction is used as a key reaction to construct these acetylene-linked denrimers. Compounds **1**−**5**,[27] **6** and **7**,[28] and 1,3,6,8-tetraethynylpyrene (**19**)[29] are prepared according to references' methods. Coupling of **19** with an excess amount of **3** and **5** gives **T1** and **T2**, respectively, in moderate yields. **T3** and **T4** can be synthesized either by coupling of **19** with an excess amount of dendron **17** and **18**, or by coupling of intermediate **21** with an excess amount of **3** and **5**, respectively. The former reacts much more efficiently than the later. It is encouraged to use a large excess amount of **3**, **5**, **17**, or **18** to react with all the terminal acetylenes in **19** and **21** completely. The structures of the dendrimers are verified by ^1H and ^{13}C NMR spectroscopies, MALDI-TOF MS measurement, and element analysis, except for **T5**, whose mass spectrum is not obtained. All the dendrimers are highly soluble in common organic solvents, such as CH_2Cl_2, $CHCl_3$, THF, and toluene, and can form a large thin film by spin-coating their solutions. The thermal stability of the dendrimers is examined by differential scanning calorimetry (DSC) and thermogravimetric analysis (TGA) in N_2 at a heating rate of 20 deg/min, and the results are listed in Table 1. All the denrimers exhibit high glass transition temperatures (T_g). **T3** exhibits the highest value of 174 °C, while **T2** shows the lowest value of 128 °C. A moderate value of 161 °C is observed in **T5** with the largest size, indicating that there is no correlation between the dendrimer size and the T_g value. All the dendrimers enjoy high thermal stability, with decomposition temperatures (T_d, corresponding to a 5% weight loss) in the range of 425−442 °C. Such high T_g and T_d values of the dendrimers are advantages for OLED applications, which help to enhance device stability and lifetime.

2.2. Visualization and Simulation. Structures of dendrimer **T1**−**T5** are optimized by the MM^+ method in the Gaussian 03 program. Figure 1 displays the molecular models. **T1** and **T2** exhibit an X shape with a calculated length of about 5 and 7 nm, respectively. **T3**, **T4**, and **T5** show a dense "pancake-like" shape with a calculated diameter of about 9, 11, and 14 nm, respectively. Because **T5** possesses many arms at its periphery, its dendrons are distorted in order to avoid the involved steric crowdedness. The whole molecule thus is "thick" in the periphery and "thin" in the center, which hampers the pyrene ring from another molecule to get close to form excimer. Since molecules with smaller dendrons are more planar and "smooth", efficient isolation of one pyrene ring from the others is relatively difficult.

2.3. Optical Properties. The absorption spectra of the dendrimers in CH_2Cl_2 and in thin neat films are illustrated in Figure 2, and the relevant data are listed in Table 1. All the dendrimers show two prominent absorption bands with maxima at about 500 and 390 nm, respectively. Since 1,3,6,8-tetrakis(phenylethynyl)pyrene absorbs strongly at 475 nm with a weak band in the range of 350−400 nm,[21a,29] the first absorption band should be ascribed to $\pi-\pi^*$ transitions of the core (pyrene ring with a certain extension). The molar absorption coefficient (ε) is insensitive to the generation number, probably because the peripheral fluorene/carbazole dendrons do not efficiently conjugated to the core through 3,6,9-carbazole linkages.[30] The second band is assigned to the absorption of fluorene/carbazole dendrons, and the molar absorption coefficient (ε) increases with the generation number. As **T2** possesses a larger conjugation system than **T1**, it exhibits a slightly red-shifted (2 nm) absorption maximum and larger ε. Similarly, the second absorption band of **T4** is red-shifted by 11 nm as fluorene units accumulate in the dendrons in comparison with that of **T3**. Solid state absorption spectra of the dendrimers are similar to those in solutions but for a slight shift to longer wavelength. Since the dendrons of **T1**−**T5** absorb at lower wavelength than the pyrene core, they may serve as antennas for energy injection and transfer as well as spacers between chromophores to suppress aggregates or excimer formation.

The PL spectra of the dendrimers in dilute CH_2Cl_2 solutions ($\sim 1 \times 10^{-6}$ M) and in thin neat films are displayed in Figure 3. The wavelength of excitation light is 380 nm. In solutions, these dendrimers exhibit a strong generation-independent emission peak at ~522 nm with a narrow full width at half-emission maximum (fwhm) of ~25 nm, which is attributed to the

(27) Zhao, Z.; Xu, X.; Xu, L.; Yu, G.; Lu, P.; Liu, Y. *Synth. Met.* **2007**, *157*, 414.
(28) Zhang, Q.; Chen, J.; Cheng, Y.; Wang, L.; Ma, D.; Jing, X.; Wang, F. *J. Mater. Chem.* **2004**, *14*, 895.
(29) Venkataramana, G.; Sankararaman, S. *Eur. J. Org. Chem.* **2005**, 4162.
(30) (a) Loiseau, F.; Campagna, S.; Hameurlaine, A.; Dehaen, W. *J. Am. Chem. Soc.* **2005**, *127*, 11352. (b) Xu, T.; Lu, R.; Liu, X.; Zheng, X.; Qiu, X.; Zhao, Y. *Org. Lett.* **2007**, *9*, 797. (c) Brunner, K.; Dijken, A.; Börner, H.; Bastiaansen, J. J. A. M.; Kiggen, K. M. M.; Langeveld, B. M. W. *J. Am. Chem. Soc.* **2004**, *126*, 6035. (d) Li, Y.; Ding, J.; Day, M.; Tao, Y.; Lu, J.; D'iorio, M. *Chem. Mater.* **2004**, *16*, 2165.

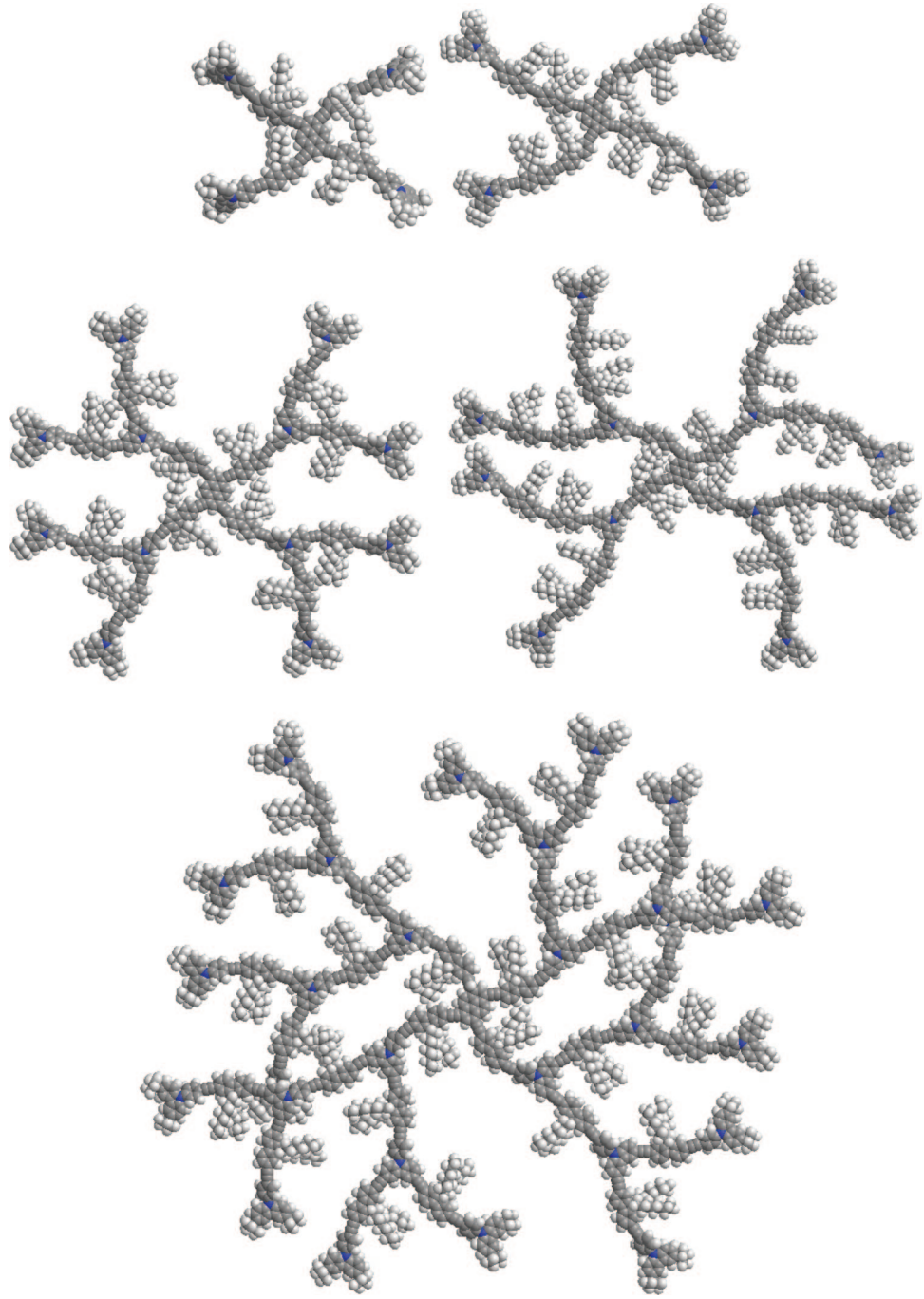

FIGURE 1. Molecular models of **T1**−**T5** optimized by the MM^+ method in the Gaussian 03 program.

emission from the core.[29] The emission changes little with different excitation wavelength. When the dendrimers are excited in the absorption range of the dendrons at 350−390 nm, the emission spectra are dominated by strong emission from the core with weak dendron emission at 400−450 nm.[22a] When the solutions are excited in the absorption range of the core at 450−500 nm, only weak emission is recorded. The observation of strong core emission upon excitation of fluorene/carbazole dendrons suggests the occurrence of efficient intramolecular singlet energy transfer.[16] One noticeable thing is that dendrimer **T4** exhibits the strongest dendron emission among the dendrimers, which might be due to its incomplete energy transfer in longer conjugated arms.

In thin films, **T1** and **T2** emit at 531 and 532 nm with shoulder peaks at 572 and 568 nm, respectively, which are red-shifted from those in the solutions by ∼8 nm. On the contrary, **T3** and **T4** exhibit a much broader and strongly red-shifted emission at ∼560 nm. A possible reason for this difference is that dendrimers **T3** and **T4** are more stretched and "pancake-like" structures, and thus are prone to close, face-to-face stacking that leads to the aggregates and/or excimer formation of pyrene rings. **T5** shows only one emission peak at 530 nm and the excimer formation between pyrene rings seems to be suppressed by its large, stiff, and twisted dendrons.

All the dendrimers are highly fluorescent in both solutions and solid states. The PL quantum yields of the dendrimers are

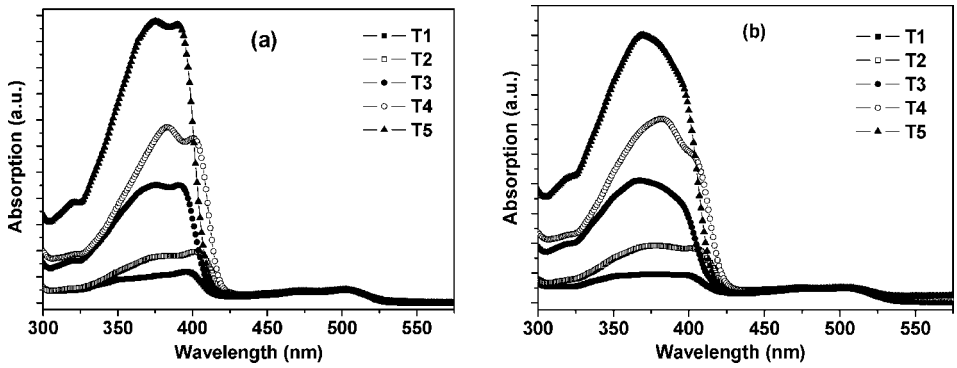

FIGURE 2. Absorption spectra of dendrimers in dilute CH_2Cl_2 solutions (a) and in thin neat films (b).

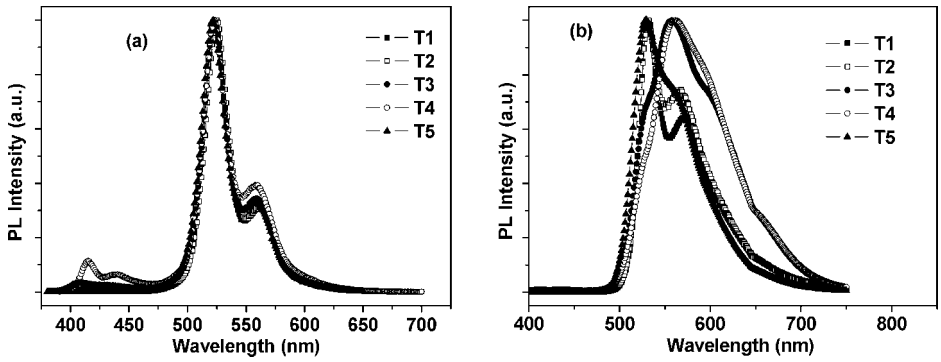

FIGURE 3. PL spectra of dendrimers in dilute CH_2Cl_2 solutions (a) and in thin neat films (b).

measured in degassed cyclohexane solutions by using 9,10-bis(phenylethynyl)anthracene ($\Phi = 1.0$ in cyclohexane)[31] as a standard. As show in Table 1, the quantum yields of the dendrimers are much higher than that of 1,3,6,8-tetrakis(phenylethynyl)pyrene (0.18).[29] On the other hand, the quantum yield declines with generation increases seen from **T1** (0.58), **T3** (0.48), and **T5** (0.42). This is possibly due to incomplete energy transfer, particularly in stiff **T5**, even though its largest dendrons have the best photon-harvesting ability. The energy transfer efficiency may decrease as generation increases because some of the arms are far away from the core.[16] **T2** exhibits a highest quantum yield of 0.65, which may be due to its better conjugation system in which excited energy can be transferred to the core efficiently.

2.4. Film Morphology. The impact of generation on the film morphology of dendrimers is investigated. The films are prepared by spin-coating *p*-xylene solutions of dendrimers (2 wt %) on SiO_2/Si substrate at a spin speed of 2000 rpm. To obtain uniform thin films, the films are prepared by spin-coating once, because during every secondary spin-coating, some of the dendrimer molecules will be redissolved by the added solution, which produces locally higher concentrations (near the interface). The film morphology is investigated by atomic force microscopy (AFM) at a tapping mode. Generally, all the films are amorphous with a fairly smooth surface, suggesting that these dendrimers possess good film-forming ability. Figure 4 compares the film morphology of **T3** and **T5**. The surface of the **T5** film appears to be rougher than that of the **T3** film, which should be attributed to **T5**'s large, rigid, and twisted dendrons. The obvious difference in film morphology arising from different generations may, in most cases, have influence on their device performances.

2.5. Electrochemical Property. The electrochemical property of dendrimers was investigated by cyclic voltammetry carried out in 0.1 M $Bu_4NPF_6-CH_2Cl_2$ at a scan rate of 100 mV/s. The cyclic voltammograms are shown in Figure 5, and the relative data of energy levels are listed in Table 1. There is one poorly resolved reversible oxidation peak observed for each dendrimer. On the basis of roughly evaluated onset oxidation potentials, the highest occupied molecular orbital (HOMO) energy levels of dendrimers are estimated in the range of −5.98 to −5.76 eV (HOMO = E^{ox}_{onset} + 4.4 eV). The lowest unoccupied molecular orbital (LUMO) energy levels are ranged from −3.62 to −3.41 eV, calculated from the HOMO energy level and energy band gap (E_g) determined from the UV−vis absorption threshold (LUMO = HOMO − E_g eV). The obtained data seem to suggest that dendrimers with higher generation possess higher energy levels.

2.6. Electroluminescence. 2.6.1. Generation Effect. The generation effect on the EL property of the dendrimers is investigated in single-layer devices with a configuration of ITO (120 nm)/PEDOT (25 nm)/dendrimer/Cs_2CO_3 (1 nm)/Al (100 nm). The details of device fabrication can be found elsewhere.[32] The dendrimer films are fabricated by a spin-coating speed ranging from 800 to 3500 rpm from *p*-xylene solutions containing 4 wt % **T1**, 4 wt % **T2**, 2.5 wt % **T3**, 2 wt % **T4**, and 2 wt % **T5**, respectively. Figure 6 displays the EL spectra of dendrimers. The EL spectra of the dendrimers are broader than but resemble their PL spectra in thin neat films, revealing that both PL and EL originate from the same radiative-decay process of singlet excitons.[33] **T1** and **T2** show greenish yellow EL at 576 and 572 nm with Commission Internationale d'Eclairage (CIE) chromaticity coordinates of (0.48, 0.51) and

(31) Berlman, I. B. *Handbook of Fluorescence Spectra of Aromatic Molecules*; Academic Press: New York, 1971.

(32) Huang, J.; Li, G.; Wu, E.; Xu, Q.; Yang, Y. *Adv. Mater.* **2006**, *18*, 114.

(33) Shih, P.-I.; Tseng, Y.-H.; Wu, F.-I.; Dixit, A. K.; Shu, C.-F. *Adv. Funct. Mater.* **2006**, *16*, 1582.

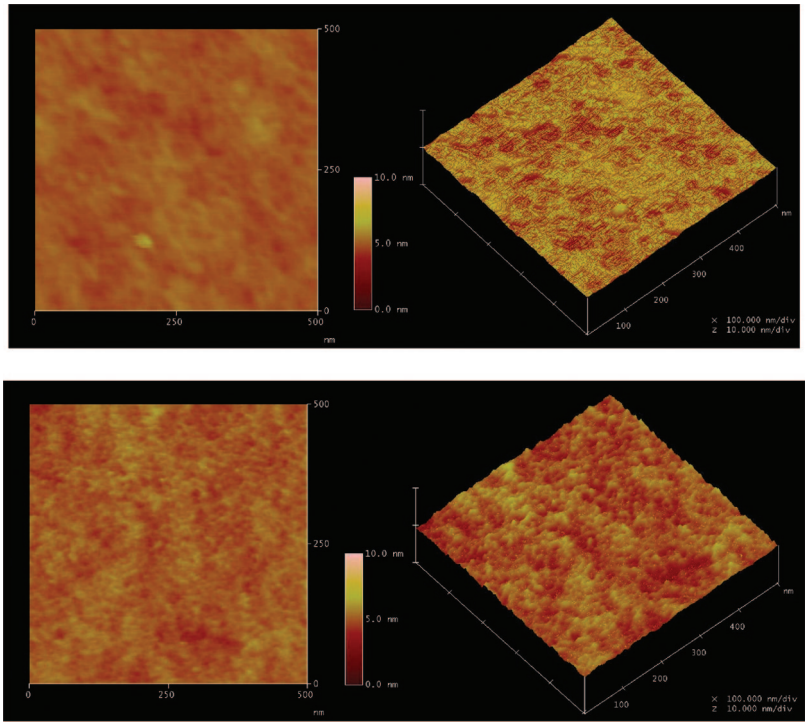

FIGURE 4. AFM images of **T3** film (up) and **T5** film (down).

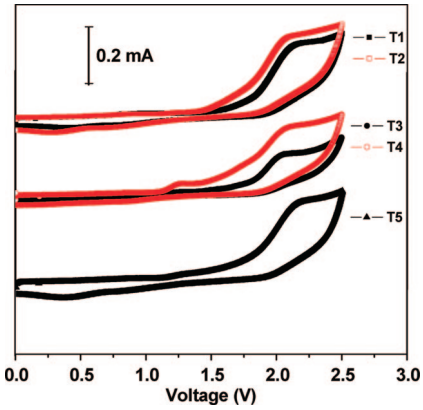

FIGURE 5. Cyclic voltammograms of dendrimers **T1**−**T5** in 0.1 M Bu_4NPF_6−CH_2Cl_2, scan rate 100 mV/s.

(0.47, 0.52), respectively. **T3** and **T4** show yellow EL (CIE: 0.49, 0.50 for **T3**, and 0.51, 0.49 for **T4**) at 560 nm. On the other hand, **T5** exhibits a narrow yellowish green (CIE: 0.39, 0.59) EL at 530 nm with a weak emission at ∼560 nm, which is comparable to its PL in both solutions and solid states. Since materials with repeating fluorene units have been reported to undergo a process of alignment in an electric field and small-sized molecules with high mobility are prone to form aggregates,[34] the broader and redder EL of **T1** and **T2** may be due to further aggregation of their molecules, which results in close stacking of pyrene rings and formation of excimers upon electric excitation. Thus, dendrons with two or more generations seem to be required to achieve efficient isolation of the core of this kind of dendrimers in the electronic field.

Generally, aggregation and/or excimer formation will quench the PL and EL efficiencies due to excited energy loss through intermolecular interaction. Interestingly, we find that a certain extent of intermolecular interaction can improve the device efficiency. Figure 7 shows the current density−voltage−luminance ($J-V-L$) characteristics and current efficiency curves of a **T3**-based device as an example (for device performances of other dendrimers, please refer to the Supporting Information). When the dendrimer films are prepared under comparable spin-coating speeds, a **T3**-based device exhibits best performance characteristics. For example, at a speed of 1500 rpm, a **T3**-based device exhibits a maximum brightness of 5590 cd/m^2 at 16 V with a high current efficiency of 2.67 cd/A at 8.6 V. Moreover, Figure 8 compares the external quantum efficiency curves of the most efficient devices based on **T1**−**T5**. A **T3**-based device shows the highest external quantum efficiency with a peak value of 0.86%. While the peak values of **T1**-, **T2**-, **T4**-, and **T5**-based devices are only 0.09%, 0.23%, 0.57%, and 0.49%, respectively. Such findings are in contrast to the general belief that a dendrimer with a higher generation can improve the device performances.[5g,9a,10b] The best performance of **T3** indicates the distinctive effect of intermolecular interaction is offset by the constructive one. As mentioned before, strong intermolecular $\pi-\pi$ interaction between dendrimer molecules is undesirable because it results in decreased efficiency and red-shifted emission. On the other hand, such strong interaction can lead to better hole transport between dendrons, as well as carrier transport through a hopping pathway between pyrene rings. Thus red-shifted emission with high efficiency is observed. Although the further increase in generation as well as dendron size hinders close intramolecular $\pi-\pi$ stacking, it has, however, lowered carrier-transporting efficiency. The inferior performance but blue-shifted emission of **T5** with respect to that of **T3** is a good indicator.

2.6.2. Effect of Spin Speed. Since spin-coating has become one of the most commonly used techniques for thin polymer film preparation, the relationships between fabrication conditions (spin speed, solvent, concentration, etc.) and electronic and

(34) (a) Weinfurtner, K.-H.; Fujikawa, H.; Tokito, S.; Taga, Y. *Appl. Phys. Lett.* **2000**, *76*, 2502. (b) Bradley, D. D. C.; Grell, M.; Long, X.; Mellor, H.; Grice, A. *Proc. SPIE* **1998**, *3145*, 254.

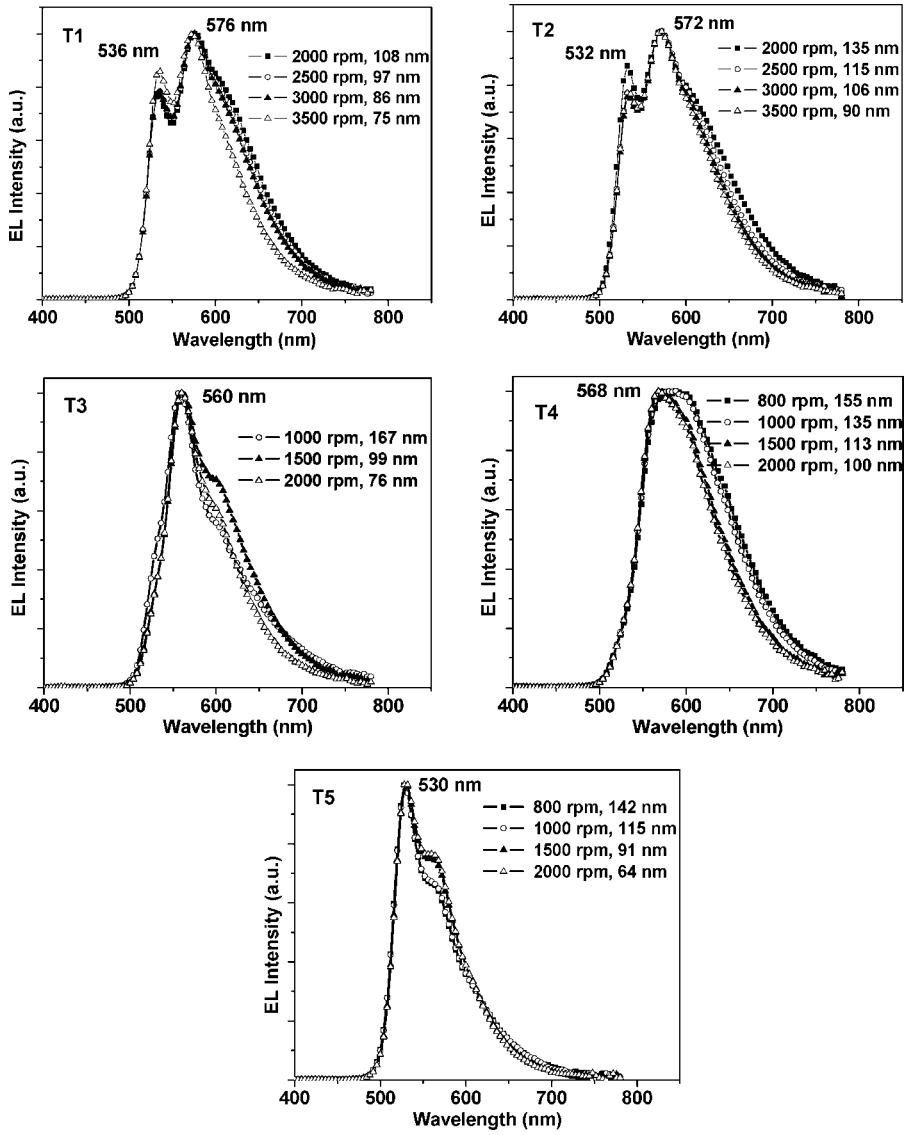

FIGURE 6. EL spectra of dendrimer devices with a configuration of ITO/PEDOT/**T1**−**T5**/Cs_2CO_3/Al.

photonic properties of polymer films as well as device performances have been extensively studied.[35,36] Generally, low spin speed results in thick films and thermodynamically favorable aggregation of molecules because a low rate of solvent evaporation encourages strong intermolecular interaction. On the contrary, high spin speed gives thin films and the molecules may be locked in an unfavorable conformation caused by solvent molecules and the centrifugal force.[32] In the case of these dendrimers, the EL spectra and device efficiency are dependent on film microstructure and thickness controlled by spin speed. The EL spectra of **T1**, **T2**, and **T4** become narrow gradually as spin speed increases. The EL spectra of **T3** and **T5** also change with spin speed but lack correlation. The current density and brightness of devices increase as spin speed increases, particularly those of devices fabricated with large-sized dendrimers. The current efficiency is also dependent on the spin speed, and a higher efficiency can be achieved by optimization of the spin speed. Although the change in spin speed seems to be a subtle modulation in the fabrication condition, it does affect the performances of the dendrimer-based LEDs, thus offering an opportunity to further enhance their device efficiency by further engineering control.

3. Conclusions

In this work, the successfully convergent synthesis and detailed characterization of a series of solution-processable stiff dendrimers consisting of a pyrene core, carbazole/fluorene dendrons, and acetylene linkages are described. These dendrimers show good thermal stability, strong fluorescence, efficient photon-harvesting, and excellent film-forming properties. Although the acetylene-linked dendrimers are generally considered as unpromising materials for OLEDs, we found that they can show high EL efficiency in single-layer devices by proper structural and engineering controls. A good control on the degree of intermolecular interaction through generation modulation is important in order to maximize carrier transport but minimize

(35) (a) Blatchford, J. W.; Jessen, S. W.; Lin, L.-B.; Gustafson, T. L.; Fu, D.-K.; Wang, H.-L.; Swager, T. M.; MacDiarmid, A. G.; Epstein, A. J. *Phys. Rev. B* **1996**, *79*, 3299. (b) Cao, Y.; Parker, I. D.; Yu, C.; Zhang, C.; Heeger, A. J. *Nature* **1999**, *397*, 414. (c) Diaz-Garcia, M. A.; Hide, F.; Schwartz, B. J.; Andersson, M. R.; Pei, Q.; Heeger, A. J. *Synth. Met.* **1997**, *84*, 455.

(36) (a) Shi, Y.; Liu, J.; Yang, Y. *J. Appl. Phys.* **2000**, *87*, 4254. (b) Shi, Y.; Liu, J.; Yang, Y. *Macromol. Symp.* **2000**, *154*, 187. (c) Liu, J.; Shi, Y.; Ma, L.; Yang, Y. *J. Appl. Phys.* **2000**, *88*, 605.

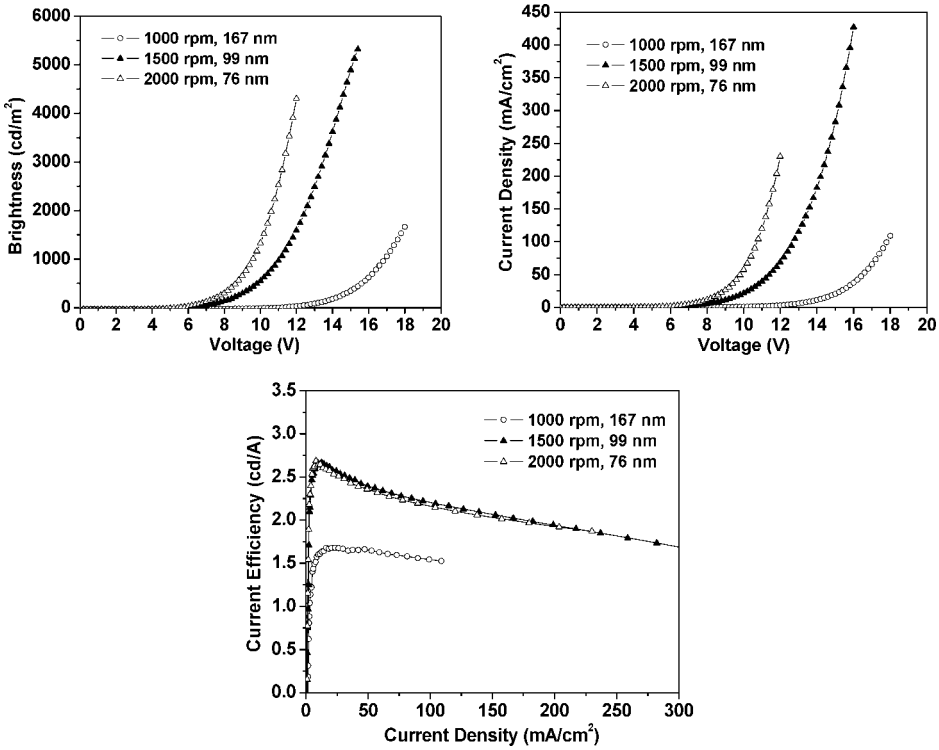

FIGURE 7. *J-V-L* characteristics and current efficiency curves of **T3**-based devices with a configuration of ITO/PEDOT/**T3**/Cs_2CO_3/Al.

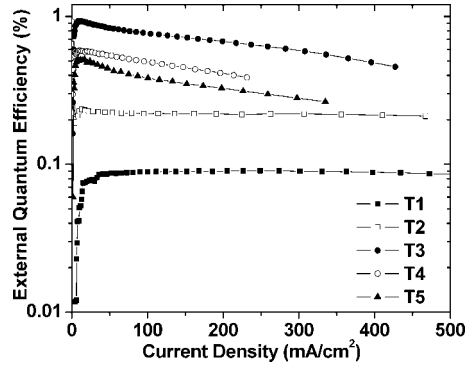

FIGURE 8. External quantum efficiency curves of the most efficient devices based on **T1**−**T5**.

excimer formation. Fabrication conditions, such as spin speed, have significant influence on EL performances. With an optimization of spin speed, the **T3**-based LED exhibits yellow EL (CIE: 0.49, 0.50) with a maximum brightness of 5590 cd/m^2 at 16 V, a high current efficiency of 2.67 cd/A at 8.6 V, and a best external quantum efficiency of 0.86%.

4. Experimental Section

4,4′-(9-(4-Bromophenyl)-9*H*-carbazole-3,6-diyl)bis(2-methylbut-3-yn-2-ol) (8). 7 (2.9 g, 5 mmol), 3-methyl-1-butyn-3-ol (1 g, 12 mmol), cuprous iodide (20 mg, 0.1 mmol), $Pd(PPh_3)_2Cl_2$ (7 mg, 0.01 mmol), PPh_3 (10 mg, 0.04 mmol), and dry triethylamine (150 mL) were placed in a 250 mL round bottle flask equipped with a Teflon covered magnetic stir bar. After the solution was purged with nitrogen for half an hour, it was refluxed under nitrogen for 12 h. The reaction mixture was evaporated under reduced pressure, and then the residue was purified through column chromatography (silica gel, hexane/dichloromethane/ethyl acetate as eluent) to afford a brown solid **8** (1.9 g, 78% yield). ^{1}H NMR ($CDCl_3$) δ 1.67 (s, 12 H), 2.20 (br, 2 H), 7.24 (d, 2 H, J = 8.5 Hz), 7.37 (d, 2 H, J = 8.5 Hz), 7.46 (dd, 2 H, J_1 = 8.5 Hz, J_2 = 1.5 Hz), 7.72 (d, 2 H, J = 8.5 Hz), 8.15 (d, 2 H, J = 1.0 Hz) ppm; ^{13}C NMR ($CDCl_3$) δ 31.9, 65.9, 82.9, 92.8, 109.9, 115.0, 121.7, 123.1, 124.3, 128.7, 130.3, 133.5, 136.1, 140.6 ppm; MALDI-TOF-MS (*m*/*z*) calcd for $C_{28}H_{24}BrNO_2$ (M^+) 485.1, found 485.0.

9-(4-Bromophenyl)-3,6-diethynyl-9*H*-carbazole (9). A mixture of **8** (1 g, 2 mmol), potassium hydroxide (2 g, 35 mmol), and 150 mL of 2-propanol was placed in a 250 mL round bottle flask equipped with a Teflon covered magnetic stir bar. After the resulting mixture was refluxed for 3 h under N_2, it was cooled to room temperature. The solution was poured into water and extracted by CH_2Cl_2. After washing by water and drying by $MgSO_4$, the solvent was then removed and the residue was purified through column chromatography (silica gel, hexane/dichloromethane as eluent). In this way, 0.64 g (86% yield) of brown, oil-like **9** was obtained. ^{1}H NMR ($CDCl_3$) δ 3.10 (s, 2 H), 7.28 (d, 2 H, J = 8.5 Hz), 7.41 (d, 2 H, J = 8.5 Hz), 7.55 (dd, 2 H, J = 8.5 Hz, J = 1.5 Hz), 7.75 (d, 2 H, J = 9.0 Hz), 8.25 (d, 2 H, J = 0.5 Hz) ppm; ^{13}C NMR ($CDCl_3$) δ 76.2, 84.6, 110.1, 114.4, 122.0, 123.1, 125.0, 128.9, 130.8, 133.6, 136.0, 141.1 ppm; MALDI-TOF-MS (*m*/*z*) calcd for $C_{22}H_{12}BrN$ (M^+) 369.0, found 370.9.

4,4′-(9-(4-((Trimethylsilyl)ethynyl)phenyl)-9*H*-carbazole-3,6-diyl)bis(2-methylbut-3-yn-2-ol) (10). 8 (2 g, 4 mmol), ethynyltrimethylsilane (0.6 g, 6 mmol), cuprous iodide (20 mg, 0.1 mmol), $Pd(Ph_3P)_4$ (11.5 mg, 0.01 mmol), PPh_3 (10.5 mg, 0.04 mmol), and dry diisopropylamine (150 mL) were placed in a 250 mL round bottle flask. After the solution was purged with nitrogen for half an hour, it was refluxed under nitrogen for 12 h. The reaction mixture was evaporated under reduced pressure, and then the residue was purified through column chromatography (silica gel, hexane/dichloromethane/ethyl acetate as eluent) to afford yellow, oil-like **10** (1.8 g, 90% yield). ^{1}H NMR ($CDCl_3$) δ 0.30 (s, 9 H), 1.68 (s, 12 H), 2.35 (br, 2 H), 7.22 (d, 2 H, J = 8.5 Hz), 7.39 (dd, 2 H, J_1 = 8.5 Hz, J_2 = 2.0 Hz), 7.43 (d, 2 H, J = 8.5 Hz), 7.67 (d, 2 H, J = 8.0 Hz), 8.12 (s, 2 H) ppm; ^{13}C NMR ($CDCl_3$) δ 0.2, 31.9, 66.0, 83.0, 92.8, 96.1, 104.2, 110.0, 115.0, 123.0, 123.2, 124.3, 126.8, 130.3, 133.8, 137.0, 140.6 ppm; MALDI-TOF-MS (*m*/*z*) calcd for $C_{33}H_{33}NO_2Si$ (M^+) 503.2, found 503.7.

4,4′-(9-(4-Ethynylphenyl)-9*H*-carbazole-3,6-diyl)bis(2-methylbut-3-yn-2-ol) (11). 10 (5 g, 10 mmol) was dissolved in 150 mL of THF containing 12 mmol of tetrabutyl ammonium fluoride (TBAF). The reaction mixture was stirred at room temperature under nitrogen overnight, then it was poured into water and extracted by CH_2Cl_2. After washing by water and drying by $MgSO_4$, the solvent was removed under reduced pressure and the residue was purified through column chromatography (silica gel, hexane/dichloromethane/ethyl acetate as eluent) to afford a white solid (4 g, 95% total yield). ^{1}H NMR ($CDCl_3$) δ 1.67 (s, 12 H), 2.22 (br, 2 H), 3.20 (s, 1 H), 7.27 (d, 2 H, J = 9.0 Hz), 7.44−7.47 (m, 4 H), 7.71 (d, 2 H, J = 8.5 Hz), 8.15 (d, 2 H, J = 1.0 Hz) ppm; ^{13}C NMR ($CDCl_3$) δ 31.9, 66.0, 78.8, 82.9, 83.0, 92.8, 110.0, 115.0, 121.9, 123.2, 124.4, 126.9, 130.3, 134.0, 137.4, 140.6 ppm; MALDI-TOF-MS (*m*/*z*) calcd for $C_{30}H_{25}NO_2$ (M^+) 431.2, found 431.3.

4,4′-(9-(4-((9,9-Diheptyl-7-iodo-9*H*-fluoren-2-yl)ethynyl)phenyl)-9*H*-carbazole-3,6-diyl)bis(2-methylbut-3-yn-2-ol) (12). 11 (4.3 g, 10 mmol), 9,9-diheptyl-2,7-diiodo-9*H*-fluorene (**2**) (18.5 g, 30 mmol), cuprous iodide (100 mg, 0.5 mmol), $Pd(PPh_3)_2Cl_2$ (35 mg, 0.05 mmol), PPh_3 (50 mg, 0.2 mmol), and dry triethylamine 300 mL were placed in a 500 mL round bottle flask equipped with a Teflon covered magnetic stir bar. After the solution was purged with nitrogen for half an hour, it was refluxed under nitrogen for 4 h. The reaction mixture was filtered and the filtrate was evaporated under reduced pressure. The residue was purified through column chromatography (silica gel, hexane/dichloromethane/ethyl acetate as eluent) to afford white solid **12** (7.3 g, 80% yield). ^{1}H NMR ($CDCl_3$) δ 0.62 (br, 4 H), 0.81 (t, 6 H, J = 7.5 Hz), 1.07 (br, 12 H), 1.16−1.21 (m, 4 H), 1.68 (s, 12 H), 1.93−1.98 (m, 4 H), 2.31 (br, 2 H), 7.30 (d, 2 H, J = 8.5), 7.42−7.49 (m, 5 H), 7.53−7.56 (m, 2 H), 7.64−7.68 (m, 3 H), 7.77 (d, 2 H, J = 8.5 Hz), 8.16 (s, 2 H) ppm; ^{13}C NMR ($CDCl_3$) δ 14.3, 22.8, 23.9, 29.2, 30.1, 31.9, 32.0, 40.5, 55.7, 66.0, 83.0, 89.0, 91.9, 92.8, 93.5, 110.1, 115.0, 120.1, 121.9, 122.0, 123.2, 124.4, 126.2, 127.0, 130.3, 131.1, 132.4, 133.4, 136.3, 136.8, 140.2, 140.7, 140.9, 150.5, 153.6 ppm; MALDI-TOF-MS (*m*/*z*) calcd for $C_{57}H_{60}INO_2$ (M^+) 917.4, found 917.6.

9,9′-(4,4′-(7,7′-(9-(4-Bromophenyl)-9*H*-carbazole-3,6-diyl)bis(ethyne-2,1-diyl)bis(9,9-diheptyl-9*H*-fluorene-7,2-diyl))bis(ethyne-2,1-diyl)bis(4,1-phenylene))bis(3,6-di-*tert*-butyl-9*H*-carbazole) (13). 3 (2.2 g, 2.5 mmol), **9** (0.37 g, 1 mmol), cuprous iodide (10 mg, 0.05 mmol), $Pd(PPh_3)_2Cl_2$ (3.5 mg, 0.005 mmol), PPh_3 (5 mg, 0.02 mmol), and dry triethylamine (150 mL) were placed in a 250 mL round bottle flask equipped with a Teflon covered magnetic stir bar. After the solution was purged with nitrogen for half an hour, it was refluxed under nitrogen for 4 h. The reaction mixture was filtered and the filtrate was evaporated under reduced pressure. The residue was purified through column chromatography (silica gel, hexane/dichloromethane as eluent) to afford pale yellow solid **13** (1.5 g, 82% yield). ^{1}H NMR ($CDCl_3$) δ 0.68 (br, 8 H), 0.82 (t, 12 H, J = 7.5 Hz), 1.09 (br, 24 H), 1.18−1.22 (m, 8 H), 1.47 (s, 36 H), 2.02−2.05 (m, 8 H), 7.34 (d, 2 H, J = 8.0 Hz), 7.40 (d, 4 H, J = 9.5 Hz), 7.44 (d, 2 H, J = 8.0 Hz), 7.48 (dd, 4 H, J_1 = 8.5 Hz, J_2 = 1.5 Hz), 7.56−7.60 (m, 12 H), 7.65 (d, 2 H, J = 9.0 Hz), 7.69−7.71 (m, 4 H), 7.74−7.78 (m, 6 H), 8.15 (d, 4 H, J = 1.5 Hz), 8.38 (s, 2 H) ppm; ^{13}C NMR ($CDCl_3$) δ 14.3, 22.8, 24.1, 29.3, 30.3, 32.1, 32.2, 35.0, 40.7, 55.5, 89.4, 89.6, 90.9, 91.5, 109.5, 110.2, 115.8, 116.5, 120.2, 120.3, 121.9, 122.0, 122.6, 123.4, 123.8, 124.0, 124.4, 126.2, 126.3, 126.6, 128.9, 130.4, 130.9, 131.1, 133.2, 133.6, 136.2, 138.3, 139.1, 140.7, 140.8, 141.2, 143.4, 151.4 ppm; MALDI-TOF-MS (*m*/*z*) calcd for $C_{132}H_{138}BrN_3$ (M^+) 1844.0, found 1844.8.

9,9′-(4,4′-(7,7′-(7,7′-(9-(4-Bromophenyl)-9*H*-carbazole-3,6-diyl)bis(ethyne-2,1-diyl)bis(9,9-diheptyl-9*H*-fluorene-7,2-diyl))-bis(ethyne-2,1-diyl)bis(9,9-diheptyl-9*H*-fluorene-7,2-diyl))bis-(ethyne-2,1-diyl)bis(4,1-phenylene))bis(3,6-di-*tert*-butyl-9*H*-carbazole) (14). The procedure was analogous to that described for **13** (78% yield, a pale green solid). ^{1}H NMR ($CDCl_3$) δ 0.65 (br, 16 H), 0.82 (t, 24 H, J = 7.5 Hz), 1.08 (br, 48 H), 1.18−1.22 (m, 16 H), 1.47 (s, 36 H), 2.02−2.04 (m, 16 H), 7.40 (d, 4 H, J = 9.0 Hz), 7.49 (dd, 6 H, J_1 = 9.0 Hz, J_2 = 2.0 Hz), 7.56−7.61 (m, 22 H), 7.67 (dd, 2 H, J_1 = 8.5 Hz, J_2 = 1.5 Hz), 7.71 (d, 8 H, J = 8.0 Hz), 7.77−7.79 (m, 6 H), 8.15 (d, 4 H, J = 2.0 Hz), 8.38 (d, 2 H, J = 1.0 Hz) ppm; ^{13}C NMR ($CDCl_3$) δ 14.3, 22.8, 24.0, 29.3, 30.3, 32.1, 32.3, 35.0, 40.7, 40.8, 55.6, 89.5, 89.6, 90.9, 91.0, 91.1, 91.5, 109.5, 110.2, 115.8, 116.6, 120.2, 120.3, 122.0, 122.2, 122.4, 122.6, 123.4, 123.8, 124.0, 124.4, 126.1, 126.2, 126.3, 126.7, 128.9, 130.4, 130.9, 131.0, 131.1, 133.2, 133.6, 136.2, 138.3, 139.1, 140.8, 140.9, 141.1, 141.2, 143.5, 151.4, 151.4 ppm; MALDI-TOF-MS (*m*/*z*) calcd for $C_{190}H_{210}BrN_3$ (M^+) 2612.6, found 2613.1.

9,9′-(4,4′-(7,7′-(9-(4-Ethynylphenyl)-9*H*-carbazole-3,6-diyl)bis(ethyne-2,1-diyl)bis(9,9-diheptyl-9*H*-fluorene-7,2-diyl))bis(ethyne-2,1-diyl)bis(4,1-phenylene))bis(3,6-di-*tert*-butyl-9*H*-carbazole) (15). 13 (3.7 g, 2 mmol), 3-methyl-1-butyn-3-ol (0.2 g, 2.4 mmol), cuprous iodide (20 mg, 0.1 mmol), $Pd(Ph_3P)_4$ (11.5 mg, 0.01 mmol), Ph_3P (10.5 mg, 0.04 mmol), and dry diisopropylamine (150 mL) were placed in a 250 mL round bottle flask equipped with a Teflon covered magnetic stir bar. After the solution was purged with nitrogen for half an hour, it was refluxed under nitrogen for 12 h. The reaction mixture was evaporated under reduced pressure and the residue was purified through column chromatography (silica gel, hexane/ethyl acetate as eluent) to afford a pale yellow solid. Then the obtained solid, potassium hydroxide (1 g, 17 mmol), and 150 mL of 2-propanol were placed in a 250 mL round bottle flask. After the resulting mixture was refluxed for 3 h under N_2, it was cooled to room temperature. The solution was then poured into water and extracted by CH_2Cl_2. After washing by water and drying by $MgSO_4$, the solvent was removed and the residue was purified through column chromatography (silica gel, hexane/dichloromethane as eluent). In this way, 2.3 g (65% total yield) of **15** (a pale yellow solid) was obtained. ^{1}H NMR ($CDCl_3$) δ 0.67 (br, 8 H), 0.82 (t, 12 H, J = 7.5 Hz), 1.09 (br, 24 H), 1.17−1.21 (m, 8 H), 1.47 (s, 36 H), 2.02−2.05 (m, 8 H), 3.21 (s, 1 H), 7.40 (d, 6 H, J = 9.0 Hz), 7.48 (dd, 4 H, J_1 = 8.5 Hz, J_2 = 2.0 Hz), 7.56−7.61 (m, 14 H), 7.67 (dd, 2 H, J_1 = 8.5 Hz, J_2 = 1.5 Hz), 7.71 (dd, 4 H, J_1 = 8.0 Hz, J_2 = 2.5 Hz), 7.76−7.78 (m, 6 H), 8.15 (d, 4 H, J = 1.5 Hz), 8.39 (s, 2 H) ppm; ^{13}C NMR ($CDCl_3$) δ 14.3, 22.6, 24.0, 29.3, 30.3, 32.1, 32.3, 35.0, 40.7, 55.5, 78.8, 82.9, 89.4, 89.6, 90.9, 91.5, 109.5, 110.3, 115.8, 116.5, 120.2, 120.3, 121.9, 122.0, 122.6, 123.5, 123.8, 124.0, 124.4, 126.2, 126.3, 126.7, 127.1, 130.4, 130.9, 131.1, 133.2, 134.1, 137.4, 138.3, 139.1, 140.7, 140.8, 141.2, 143.4, 151.4 ppm; MALDI-TOF-MS (*m*/*z*) calcd for $C_{134}H_{139}N_3$ (M^+) 1790.1, found 1791.2.

9,9′-(4,4′-(7,7′-(7,7′-(9-(4-Ethynylphenyl)-9*H*-carbazole-3,6-diyl)bis(ethyne-2,1-diyl)bis(9,9-diheptyl-9*H*-fluorene-7,2-diyl))-bis(ethyne-2,1-diyl)bis(9,9-diheptyl-9*H*-fluorene-7,2-diyl))bis-(ethyne-2,1-diyl)bis(4,1-phenylene))bis(3,6-di-*tert*-butyl-9*H*-carbazole) (16). The procedure was analogous to that described for **15** (47% yield, a pale yellow solid). ^{1}H NMR ($CDCl_3$) δ 0.64 (br, 16 H), 0.82 (t, 24 H, J = 7.5 Hz), 1.08 (br, 48 H), 1.18−1.22 (m, 16 H), 1.47 (s, 36 H), 2.02−2.04 (m, 16 H), 3.22 (s, 1 H), 7.41 (d, 6 H, J = 8.5 Hz), 7.49 (dd, 4 H, J_1 = 9.0 Hz, J_2 = 2.0 Hz), 7.56−7.61 (m, 22 H), 7.67 (dd, 2 H, J_1 = 8.5 Hz, J_2 = 1.0 Hz), 7.71 (d, 8 H, J = 8.0 Hz), 7.77−7.79 (m, 6 H), 8.15 (d, 4 H, J = 1.5 Hz), 8.39 (s, 2 H) ppm; ^{13}C NMR ($CDCl_3$) δ 14.3, 22.8, 24.0, 29.3, 30.3, 32.1, 32.3, 35.0, 40.7, 40.8, 55.5, 78.8, 82.9, 89.5, 89.6, 90.9, 91.0, 91.1, 91.5, 109.5, 110.3, 115.8, 116.5, 120.2, 120.3, 120.3, 122.00, 122.1, 122.2, 122.3, 122.6, 123.5, 123.8, 124.0, 124.4, 126.1, 126.2, 126.3, 126.7, 127.1, 130.4, 130.9, 131.0, 131.1, 133.2, 134.1, 137.5, 138.3, 139.1, 140.7, 140.8, 140.9, 141.1, 141.2, 143.4, 151.4 ppm; MALDI-TOF-MS (*m*/*z*) calcd for $C_{192}H_{211}N_3$ (M^+) 2558.7, found 2559.3.

9,9′-(4,4′-(7,7′-(9-(4-((9,9-Diheptyl-7-iodo-9*H*-fluoren-2-yl)ethynyl)phenyl)-9*H*-carbazole-3,6-diyl)bis(ethyne-2,1-diyl)bis(9,9-diheptyl-9*H*-fluorene-7,2-diyl))bis(ethyne-2,1-diyl)bis(4,1-phenylene))bis(3,6-di-*tert*-butyl-9*H*-carbazole) (17). The procedure was analogous to that described for **12** (73% yield, a pale yellow solid). ^{1}H NMR ($CDCl_3$) δ 0.67 (br, 12 H), 0.81−0.84 (m, 18 H), 1.08−1.10 (m,

36 H), 1.18−1.22 (m, 12 H), 1.47 (s, 36 H), 1.95−2.06 (m, 12 H), 7.40 (d, 4 H, J = 9.0 Hz), 7.44 (d, 2 H, J = 8.5 Hz), 7.49 (dd, 4 H, J_1 = 8.5 Hz, J_2 = 2.0 Hz), 7.55−7.62 (m, 18 H), 7.68−7.69 (m, 4 H), 7.72 (dd, 4 H, J_1 = 8.5 Hz, J_2 = 2.0 Hz), 7.78 (d, 4 H, J = 6.0 Hz), 7.83 (d, 2 H, J = 8.5 Hz), 8.15 (d, 4 H, J = 2.0 Hz), 8.40 (d, 2 H, J = 1.5 Hz) ppm; ^{13}C NMR ($CDCl_3$) δ 14.3, 22.8, 24.0, 29.3, 30.3, 32.1, 32.3, 35.0, 40.7, 55.5, 78.8, 82.9, 89.4, 89.6, 90.9, 91.5, 109.5, 110.3, 115.8, 116.5, 120.2, 120.3, 121.9, 122.0, 122.6, 123.5, 123.8, 124.0, 124.4, 126.2, 126.3, 126.7, 127.1, 130.4, 130.9, 131.1, 133.2, 134.2, 137.4, 138.3, 139.2, 140.7, 140.8, 141.2, 143.4, 151.4 ppm; MALDI-TOF-MS (*m*/*z*) calcd for $C_{161}H_{174}IN_3$ (M^+) 2276.3, found 2150.0 ($M^+ - I$). Anal. Calcd for $C_{161}H_{174}IN_3$: C, 84.89; H, 7.70; N, 1.84. Found: C, 84.91; H, 7.74; N, 1.82.

9,9′-(4,4′-(7,7′-(7,7′-(9-(4-((9,9-Diheptyl-7-iodo-9*H*-fluoren-2-yl)ethynyl)phenyl)-9*H*-carbazole-3,6-diyl)bis(ethyne-2,1-diyl)-bis(9,9-diheptyl-9*H*-fluorene-7,2-diyl))bis(ethyne-2,1-diyl)bis(9,9-diheptyl-9*H*-fluorene-7,2-diyl))bis(ethyne-2,1-diyl)bis(4,1-phenylene))bis(3,6-di-*tert*-butyl-9*H*-carbazole) (18). The procedure was analogous to that described for **12** (67% yield, a pale yellow solid). ^{1}H NMR ($CDCl_3$) δ 0.65 (br, 20 H), 0.80−0.84 (m, 32 H), 1.08 (br, 58 H), 1.18−1.21 (m, 20 H), 1.47 (s, 36 H), 1.95−2.04 (m, 20 H), 7.40 (d, 4 H, J = 8.5 Hz), 7.45 (d, 2 H, J = 8.5 Hz), 7.49 (dd, 4 H, J_1 = 8.5 Hz, J_2 = 2.0 Hz), 7.55−7.62 (m, 26 H), 7.68−7.72 (m, 12 H), 7.78 (d, 4 H, J = 8.5 Hz), 7.83 (d, 2 H, J = 8.0 Hz), 8.15 (d, 4 H, J = 1.5 Hz), 8.40 (s, 2 H) ppm; ^{13}C NMR ($CDCl_3$) δ 14.3, 22.8, 24.0, 29.2, 29.3, 30.2, 30.3, 32.0, 32.1, 32.2, 35.0, 40.5, 40.7, 40.8, 55.5, 55.7, 89.0, 89.5, 89.6, 90.9, 91.0, 91.2, 91.4, 92.0, 93.6, 109.6, 110.4, 115.7, 116.5, 120.1, 120.3, 121.9, 122.0, 122.1, 122.3, 122.6, 123.3, 123.5, 123.8, 124.0, 124.4, 126.1, 126.2, 126.6, 127.1, 130.4, 130.9, 131.0, 131.1, 131.2, 132.4, 133.2, 133.5, 136.3, 136.8, 138.3, 139.1, 140.2, 140.7, 140.8, 140.9, 141.0, 141.1, 143.4, 150.6, 151.4, 153.7 ppm; MALDI-TOF-MS (*m*/*z*) calcd for $C_{219}H_{246}IN_3$ (M^+) 3044.8, found 2919.7 ($M^+ - I$). Anal. Calcd for $C_{219}H_{246}IN_3$: C, 86.32; H, 8.14; N, 1.38. Found: C, 86.12; H, 8.34; N, 1.29.

4,4′,4″,4‴,4⁗,4⁗′-(9,9′,9″-(4,4′,4″-(7,7′,7″-(8-((7-((4-(3,6-Bis(3-hydroxy-3-methylbut-1-ynyl)-9*H*-carbazol-9-yl)phenyl)-ethynyl)-9,9-diheptyl-9*H*-fluoren-2-yl)ethynyl)pyrene-1,3,6-triyl) tris(ethyne-2,1-diyl)tris(9,9-diheptyl-9*H*-fluorene-7,2-diyl))tris(ethyne-2,1-diyl)tris(4,1-phenylene))tris(9*H*-carbazole-9,6,3-triyl))hexakis(2-methylbut-3-yn-2-ol) (20). The procedure was analogous to that described for **12** (58% yield, an orange-red solid). ^{1}H NMR ($CDCl_3$) δ 0.74 (br, 16 H), 0.83 (t, 24 H, J = 7.5 Hz), 1.13 (br, 48 H), 1.20−1.25 (m, 16 H), 1.69 (s, 48 H), 2.11 (br, 24 H), 7.34 (d, 8 H, J = 8.5 Hz), 7.49 (dd, 8 H, J_1 = 8.0 Hz, J_2 = 2.0 Hz), 7.54 (d, 8 H, J = 8.5 Hz), 7.60−7.62 (m, 8 H), 7.74−7.82 (m, 24 H), 8.18 (d, 8 H, J = 1.0 Hz), 8.57 (s, 2 H), 8.89 (s, 4 H) ppm; ^{13}C NMR ($CDCl_3$) δ 14.3, 22.9, 24.1, 29.3, 30.3, 31.9, 32.1, 40.7, 55.7, 66.0, 83.0, 88.6, 89.2, 92.0, 92.8, 97.6, 110.1, 115.1, 119.4, 120.5, 120.5, 122.0, 122.3, 123.3, 124.4, 124.6, 126.3, 127.0, 127.2, 130.3, 131.3, 131.4, 132.0, 133.4, 134.3, 136.9, 140.7, 141.2, 141.3, 151.5, 151.6 ppm; MALDI-TOF-MS (*m*/*z*) calcd for $C_{252}H_{246}N_4O_8$ (M^+) 3455.9, found 3458.8. Anal. Calcd for $C_{252}H_{246}N_4O_8$: C, 87.51; H, 7.17; N, 1.62. Found: C, 87.46; H, 7.19; N, 1.51.

1,3,6,8-Tetrakis((7-((4-(3,6-diethynyl-9*H*-carbazol-9-yl)phenyl)ethynyl)-9,9-diheptyl-9*H*-fluoren-2-yl)ethynyl)pyrene (21). The procedure was analogous to that described for **9** (71% yield, an orange-red solid). ^{1}H NMR ($CDCl_3$) δ 0.72 (br, 16 H), 0.83 (t, 24 H, J = 7.5 Hz), 1.13 (br, 48 H), 1.20−1.23 (m, 16 H), 2.10−2.11 (m, 16 H), 3.11 (s, 8 H), 7.37 (d, 8 H, J = 8.5 Hz), 7.55−7.63 (m, 24 H), 7.75−7.83 (m, 24 H), 8.27 (d, 8 H, J = 1.0 Hz), 8.60 (s, 2 H), 8.92 (s, 4 H) ppm; ^{13}C NMR ($CDCl_3$) δ 14.3, 22.8, 24.1, 29.3, 30.3, 32.1, 40.7, 55.7, 76.2, 84.2, 88.6, 89.1, 92.1, 97.5, 110.2, 114.4, 119.4, 120.4, 120.5, 121.9, 122.2, 123.1, 123.4, 124.5, 125.0, 126.3, 127.1, 127.2, 130.8, 131.2, 131.3, 132.0, 133.5, 134.2, 136.7, 141.0, 141.2, 141.3, 151.5, 151.6 ppm; MALDI-TOF-MS (*m*/*z*) calcd for $C_{228}H_{198}N_4$ (M^+) 2291.6, found 2294.3. Anal. Calcd for $C_{228}H_{198}N_4$: C, 91.46; H, 6.67; N, 1.87. Found: C, 91.50; H, 6.68; N, 1.90.

1,3,6,8-Tetrakis((7-((4-(3,6-di-*tert*-butyl-9*H*-carbazol-9-yl)phenyl)ethynyl)-9,9-diheptyl-9*H*-fluoren-2-yl)ethynyl)pyrene (T1). The procedure was analogous to that described for **12** (79% yield, an orange-red solid). ^{1}H NMR ($CDCl_3$) δ 0.73 (br, 16 H), 0.83 (t, 24 H, J = 7.5 Hz), 1.13 (br, 48 H), 1.20−1.25 (m, 16 H), 1.48 (s, 72 H), 2.10−2.11 (m, 16 H), 7.41 (d, 8 H, J = 8.5 Hz), 7.49 (dd, 8 H, J_1 = 8.5 Hz, J_2 = 2.0 Hz), 7.58−7.62 (m, 16 H), 7.74−7.80 (m, 24 H), 8.15 (d, 8 H, J = 1.5 Hz), 8.60 (s, 2 H), 8.92 (s, 4 H) ppm; ^{13}C NMR ($CDCl_3$) δ 14.3, 22.9, 24.1, 29.3, 30.3, 32.1, 32.3, 35.0, 40.7, 55.7, 88.6, 89.6, 91.4, 97.6, 116.6, 119.5, 120.4, 120.5, 122.0, 122.6, 123.9, 124.0, 124.6, 126.3, 126.7, 127.3, 131.2, 131.4, 132.1, 133.3, 138.4, 139.2, 141.1, 141.4, 143.5, 151.5, 151.7 ppm; MALDI-TOF-MS (*m*/*z*) calcd for $C_{244}H_{262}N_4$ (M^+) 3248.1, found 3247.9. Anal. Calcd for $C_{244}H_{262}N_4$: C, 90.15; H, 8.12; N, 1.72. Found: C, 90.34; H, 8.19; N, 1.44.

1,3,6,8-Tetrakis((7-((7-((4-(3,6-di-*tert*-butyl-9*H*-carbazol-9-yl)phenyl)ethynyl)-9,9-diheptyl-9*H*-fluoren-2-yl)ethynyl)-9,9-diheptyl-9*H*-fluoren-2-yl)ethynyl)pyrene (T2). The procedure was analogous to that described for **12** (74% yield, an orange-red solid). ^{1}H NMR ($CDCl_3$) δ 0.66−0.71 (m, 32 H), 0.81−0.84 (m, 48 H), 1.09−1.12 (m, 96 H), 1.19−1.23 (m, 32 H), 1.48 (s, 72 H), 2.04−2.10 (m, 32 H), 7.41 (d, 8 H, J = 9.0 Hz), 7.49 (dd, 8 H, J_1 = 8.5 Hz, J_2 = 2.5 Hz), 7.57−7.64 (m, 32 H), 7.71−7.73 (m, 12 H), 7.76−7.82 (m, 20 H), 8.15 (d, 8 H, J = 2.0 Hz), 8.60 (s, 2 H), 8.93 (s, 4 H) ppm; ^{13}C NMR ($CDCl_3$) δ 14.3, 14.3, 22.9, 24.0, 29.3, 30.3, 32.1, 32.3, 35.0, 40.7, 40.8, 55.6, 55.7, 88.5, 89.5, 91.1, 91.2, 91.4, 97.6, 109.5, 116.6, 119.5, 120.3, 120.4, 122.0, 122.1, 122.3, 122.5, 123.8, 124.0, 126.3, 126.7, 131.0, 131.1, 131.3, 132.1, 133.2, 138.3, 139.1, 140.9, 141.0, 141.1, 141.5, 143.5, 151.4, 151.5, 151.6 ppm; MALDI-TOF-MS (*m*/*z*) calcd for $C_{360}H_{406}N_4$ (M^+) 4785.2, found 4785.3. Anal. Calcd for $C_{360}H_{406}N_4$: C, 90.29; H, 8.54; N, 1.17. Found: C, 90.17; H, 8.71; N, 1.09.

1,3,6,8-Tetrakis((7-((4-(3,6-bis((7-((4-(3,6-di-*tert*-butyl-9*H*-carbazol-9-yl)phenyl)ethynyl)-9,9-diheptyl-9*H*-fluoren-2-yl)ethynyl)-9*H*-carbazol-9-yl)phenyl)ethynyl)-9,9-diheptyl-9*H*-fluoren-2-yl)ethynyl)pyrene (T3). The procedure was analogous to that described for **12** (65% yield, an orange-red solid). ^{1}H NMR ($CDCl_3$) δ 0.68 (br, 48 H), 0.81−0.85 (m, 72 H), 1.01−1.23 (m, 192 H), 1.47 (s, 144 H), 2.04 (br, 48 H), 7.40 (d, 16 H, J = 8.5 Hz), 7.48−7.50 (m, 20 H), 7.57−7.60 (m, 48 H), 7.63−7.65 (m, 20 H), 7.69−7.74 (m, 24 H), 7.76−7.88 (m, 40 H), 8.15 (d, 16 H, J = 8.5 Hz), 8.41 (s, 8 H), 8.63 (s, 2 H), 8.95 (s, 4 H) ppm; ^{13}C NMR ($CDCl_3$) δ 14.3, 14.4, 22.9, 24.1, 29.3, 30.3, 32.1, 32.2, 35.0, 40.7, 55.6, 55.7, 89.4, 89.6, 90.9, 91.5, 115.7, 116.5, 120.2, 120.3, 120.5, 120.5, 121.9, 122.0, 122.6, 123.5, 123.8, 124.0, 126.2, 126.3, 126.4, 126.7, 127.1, 130.4, 130.9, 131.1, 131.3, 131.4, 133.2, 133.5, 139.1, 140.7, 140.8, 141.2, 143.4, 151.4, 151.4 ppm; MALDI-TOF-MS (*m*/*z*) calcd for $C_{668}H_{702}N_{12}$ (M^+) 8892, found 8897. Anal. Calcd for $C_{668}H_{702}N_{12}$: C, 90.16; H, 7.95; N, 1.89. Found: C, 90.15; H, 7.99; N, 1.89.

1,3,6,8-Tetrakis((7-((4-(3,6-bis((7-((7-((4-(3,6-di-*tert*-butyl-9*H*-carbazol-9-yl)phenyl)ethynyl)-9,9-diheptyl-9*H*-fluoren-2-yl)ethynyl)-9,9-diheptyl-9*H*-fluoren-2-yl)ethynyl)-9*H*-carbazol-9-yl)phenyl)ethynyl)-9,9-diheptyl-9*H*-fluoren-2-yl)ethynyl)pyrene (T4). The procedure was analogous to that described for **12** (60% yield, an orange-red solid). ^{1}H NMR ($CDCl_3$) δ 0.65 (br, 80 H), 0.80−0.84 (m, 120 H), 1.09−1.20 (m, 320 H), 1.47 (s, 144 H), 2.03 (br, 80 H), 7.40 (d, 16 H, J = 8.5 Hz), 7.48−7.50 (m, 20 H), 7.57−7.76 (m, 100 H), 7.70−7.72 (m, 40 H), 7.77−7.86 (m, 40 H), 8.15 (d, 16 H, J = 1.5 Hz), 8.41 (s, 8 H), 8.63 (s, 2 H), 8.95 (s, 4 H) ppm; ^{13}C NMR ($CDCl_3$) δ 14.3, 22.9, 24.0, 29.3, 30.3, 32.1, 32.3, 35.0, 40.7, 40.8, 55.5, 55.7, 89.5, 89.6, 90.9, 91.0, 91.1, 91.4, 115.8, 116.6, 120.3, 120.3, 120.5, 121.9, 122.0, 122.1, 122.3, 122. 6, 123.5, 123.8,124.0, 126.6, 127.1, 130.4, 130.9, 131.0, 131.1, 131.3, 133.2, 133.5, 138.3, 139.1, 140.7, 140.8, 140.9, 141.1, 143.4, 151.4 ppm; MALDI-TOF-MS (*m*/*z*) calcd for $C_{900}H_{990}N_{12}$ (M^+) 11966, found

11979. Anal. Calcd for $C_{900}H_{990}N_{12}$: C, 90.26; H, 8.33; N, 1.40. Found: C, 90.21; H, 8.34; N, 1.40.

1,3,6,8-Tetrakis((7-((4-(3,6-bis((7-((4-(3,6-bis((7-((4-(3,6-di-*tert*-butyl-9*H*-carbazol-9-yl)phenyl)ethynyl)-9,9-diheptyl-9*H*-fluoren-2-yl)ethynyl)-9*H*-carbazol-9-yl)phenyl)ethynyl)-9,9-diheptyl-9*H*-fluoren-2-yl)ethynyl)-9*H*-carbazol-9-yl)phenyl)ethynyl)-9,9-diheptyl-9*H*-fluoren-2-yl)ethynyl)pyrene (T5). The procedure was analogous to that described for **12** (41% yield, an orange-red solid) except for changes in catalyst ($Pd(Ph_3P)_4$) and solvent (*i*-Pr_2NH/benzene (1/1, v/v)). ^{1}H NMR ($CDCl_3$) δ 0.68 (br, 112 H), 0.81−0.85 (m, 168 H), 1.10−1.26 (m, 448 H), 1.47 (s, 288 H), 2.05 (br, 112 H), 7.39−7.49 (m, 96 H), 7.57−7.86 (m, 296 H), 8.14 (s, 32 H), 8.40 (s, 16H), 8.42 (s, 8 H), 8.63 (s, 2 H), 8.95 (s, 4 H) ppm; ^{13}C NMR ($CDCl_3$) δ 14.3, 22.8, 24.1, 29.3, 30.3, 32.1, 32.3, 35.0, 40.7, 55.6, 89.4, 89.6, 91.0, 91.5, 109.5, 110.4, 115.8, 116.6, 120.3, 121.9, 122.0, 122.7, 123.5, 123.8, 124.0, 126.2, 126.3, 126.7, 127.1, 128.7, 128.8, 130.4, 131.0, 131.1, 132.2, 132.3, 132.4, 133.2, 133.5, 138.3, 139.2, 140.7, 140. 9, 141.2, 143.2, 143.5, 151.4 ppm. Anal. Calcd for $C_{1516}H_{1582}N_{28}$: C, 90.16; H, 7.90; N, 1.94. Found: C, 90.26; H, 7.89; N, 1.93.

Acknowledgment. P.L. thanks the National Natural Science Foundation of China (20674070) and the Natural Science Foundation of Zhejiang Province (R404109).

Supporting Information Available: General information, NMR and mass spectra of new compounds, TGA charts of dendrimers, and $J-V-L$ characteristics and current efficiency curves of devices. This material is available free of charge via the Internet at http://pubs.acs.org.

JO802237C